JCI The Journal of Clinical Investigation

Increased expression of anion transporter *SLC26A9* delays diabetes onset in cystic fibrosis

Anh-Thu N. Lam, … , Scott M. Blackman, Garry R. Cutting

J Clin Invest. 2019. https://doi.org/10.1172/JCI129833.

Research In-Press Preview Endocrinology Genetics

Graphical abstract

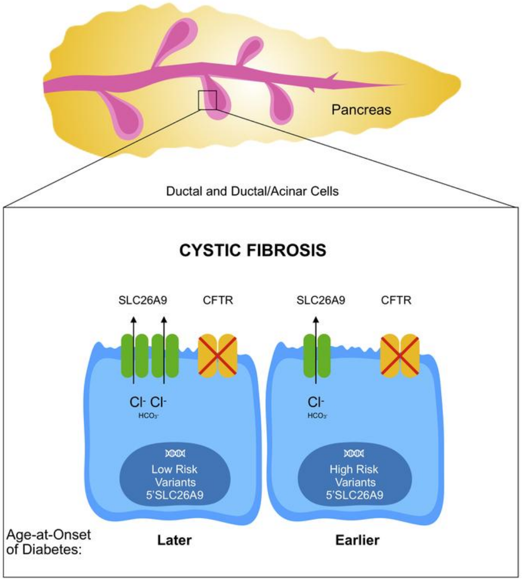
Pancreas
Ductal and Ductal/Acinar Cells
CYSTIC FIBROSIS
SLC26A9
CFTR
SLC26A9
CFTR
Cl- Cl-
HCO3-
Cl-
HCO3-
Low Risk Variants 5'SLC26A9
High Risk Variants 5'SLC26A9
Age-at-Onset of Diabetes:
Later
Earlier

Title:

Increased expression of anion transporter *SLC26A9* delays diabetes onset in cystic fibrosis

Authors:

Anh-Thu N. Lam[1], Melis A. Aksit[1], Briana Vecchio-Pagan[1,3], Celeste A. Shelton[2,4], Derek L. Osorio[1], Arianna F. Anzmann[1], Loyal A. Goff[1], David C. Whitcomb[2], Scott M. Blackman[1], Garry R. Cutting[1*].

Affiliations:

[1] McKusick-Nathans Department of Genetic Medicine, Johns Hopkins University School of Medicine, Baltimore, MD 21205, USA

[2] University of Pittsburgh, Pittsburgh, PA 15213, USA

[3] Applied Physics Laboratory, Johns Hopkins University, Laurel, MD 20723, USA

[4] Ariel Precision Medicine, 5750 Centre Avenue, Suite 270, Pittsburgh, PA 15206, USA

COI statement: "The authors have declared that no conflict of interest exists."

*Corresponding author: Garry R. Cutting, MD
Johns Hopkins University School of Medicine
Institute of Genetic Medicine
733 N. Broadway
BRB Suite 551/Room 559
Baltimore, MD, 21205
Phone: (410) 955-1773/Fax: 410-614-0213
E-mail: gcutting@jhmi.edu

Abstract

Diabetes is a common complication of cystic fibrosis (CF) that affects ~20% of adolescents and 40-50% of adults with CF. The age-at-onset of CF-related diabetes (marked by clinical diagnosis and treatment initiation) is an important measure of the disease process. DNA variants associated with age-at-onset of CFRD reside in and near *SLC26A9.* Deep sequencing of the *SLC26A9* gene in 762 individuals with CF revealed that two common DNA haplotypes formed by the risk variants account for the association with diabetes (high risk, p-value: 4.34E-3; low risk, p-value: 1.14E-3). Single-cell RNA (scRNA) sequencing indicated that *SLC26A9* is predominantly expressed in pancreatic ductal cells, and frequently co-expressed with *CFTR* along with transcription factors that have binding sites 5' of *SLC26A9*. These findings replicated upon re-analysis of scRNA data from 4 independent studies. DNA fragments derived from the 5' region of *SLC26A9* bearing variants from the low risk haplotype generated 12-20% higher levels of expression in PANC-1 and CFPAC-1 cells compared to the high risk haplotype (p-values: 2.00E-3 to 5.15E-9). Taken together, our findings indicate that an increase in *SLC26A9* expression in ductal cells of the pancreas delays the age-at-onset of diabetes, thereby suggesting a CFTR-agnostic treatment for a major complication of CF.

Introduction

Cystic fibrosis (CF), one of the most common life-limiting autosomal recessive disease in the white European population, is caused by deleterious variants in the CF transmembrane conductance regulator (*CFTR*) gene (1). Successful management of disease symptoms and malnutrition have dramatically improved CF life expectancy well into adulthood (2). As individuals with CF live longer, age-dependent complications such as diabetes are becoming more prevalent. Although only 2% of children with CF manifest CF-related diabetes (CFRD), ~20% of adolescents and 50% of adults have this complication and >90% of pancreatic insufficient individuals with CF have CFRD by age ~50 (3, 4). The development of diabetes is associated with increased morbidity (5) and mortality (3, 4). CFRD has overlapping features with type 1 and type 2 diabetes (T1D and T2D, respectively) but also displays cellular, histological, and clinical differences, thereby warranting a separate diagnostic classification (3). Reduced insulin production is observed in both T1D and CFRD, however, CFRD is not associated with the islet autoimmunity that causes T1D (6). Both CFRD and T2D shows increase in prevalence with age, a progressive defect in beta cell function, and an accumulation of amyloid polypeptide in pancreatic islets (7), and susceptibility genes for T2D also modify CFRD (8). However, in contrast to T2D, insulin sensitivity is usually normal in CFRD (3).

Since CFRD results from the progressive decline in insulin secretion, age-at-onset is an important indicator of the rate of disease progression as it marks the point at which treatment for diabetes is initiated (3). Provision of insulin improves lung function, weight and survival. There is a high degree of variability in age-at-onset of CFRD, even after accounting for the level of CFTR dysfunction (4). Studies of twins and siblings with CF indicated that variants in genes other than *CFTR* account for most of the variability in developing CFRD (9). Subsequently, a genome-wide study identified variants 5' of and within noncoding regions of *SLC26A9* that associate with age-at-onset of CFRD (8). *SLC26A9* is a member of the SLC26 family of anion transporters that functions as a WNK kinase-regulated Cl^-/HCO_3^- exchanger and Cl^- channel (and possibly as a Na^+-anion cotransporter) (10-14). Cryo-electron microscopy paired with electrophysiologic studies show that murine SLC26A9 forms homodimers that operate as rapid transporters of Cl^- as opposed to forming ion channels (15).

SLC26A9 has a diverse range of functions in vivo including acid regulation in the gastric parietal cells (16, 17), bicarbonate transport in the intestine (17) and regulation of systemic arterial pressure and chloride excretion in kidney medullary collecting duct (18). In the lung, SLC26A9 contributes to constitutive chloride secretion in the airway (19) and mucociliary clearance (20). Variants in *SLC26A9* have been previously associated with atypical CF-like lung disease and risk for asthma (20, 21) and modulation of airway response to CFTR-directed therapeutics (22, 23). *SLC26A9* has been reported to be expressed in epithelial cells of the lung and stomach and multiple other tissues including salivary gland, heart, skin, kidney, thyroid and prostate (10, 13, 24-27).

SLC26A9 is a compelling candidate as a modifier of CFRD. First, in vitro studies have shown that SLC26A9 interacts with CFTR via its STAS domain and PDZ-binding motif and that constitutive basal chloride conductance generated by SLC26A9 is regulated by CFTR (13, 19, 28). Second, the CFRD-associated variants in and near *SLC26A9* have been shown to modify prenatal exocrine pancreatic damage in CF (assessed by immunotrypsinogen levels at birth) (29) and to confer risk for CFRD by affecting exocrine pancreatic function (30, 31). Third, these variants have also been associated with risk for neonatal intestinal obstruction (MI) in CF (32), a complication that appears to be intimately linked to pancreatic exocrine insufficiency (33)*.*

Elucidating the mechanisms underlying the increasingly prevalent diabetes may be essential for continued improvement in the survival of individuals with CF. Modifiers reveal potential pathways that can be targeted for therapeutic interventions and individualized treatment of CF that can operate beyond dysfunction of the causal gene (34, 35). Importantly, a CFTR-agnostic approach may be needed for diabetes as CFTR modulators that effect dramatic improvements in lung function have not provided clear evidence of improvement in diabetic status (36-40). In this study, we investigated the genetic architecture and cellular distribution of *SLC26A9* to inform expression assays. In cell lines that reflect the native environment of *SLC26A9* in the pancreas, DNA fragments derived from the 5' region of *SLC26A9* drive reporter gene expression. Importantly, 5' variants associated with later onset of diabetes generate significantly higher levels of expression. When combined, these results imply that increased expression of SLC26A9 delays the onset of diabetes in individuals with CF. Greater understanding of the pathologic mechanism(s) provides insight that can inform molecular based treatments to delay or avert onset of diabetes.

Results

CFRD-associated variants in the *SLC26A9* are common and noncoding. To evaluate the genetic architecture of *SLC26A9*, we sequenced 47.7 kb encompassing the *SLC26A9* locus (9.9 kb 5', 30.4 kb gene and 7.4 kb 3') in 762 individuals with CF who are homozygous for the common CF-causing variant, p.Phe508del (legacy name: F508del) (see Methods for details). The sequenced region completely encompassed the variants 5' and within *SLC26A9* that are significantly associated with age-at-onset of diabetes (8). Using linear regression of martingale residuals of age-at-onset of CFRD (Figure 1A), we observed that the variants that achieved significance in the genome-wide study were associated with CFRD in this dataset ($p<0.005$) (Supplemental Table 1). rs7512462 in intron 5 had the lowest p-value, however a cluster of variants in intron 1 and 5' of *SLC26A9* were also significantly associated with age-at-onset of CFRD. All significantly CFRD-associated variants were in non-coding regions, either intronic or 5' of the gene. No individual variant was associated with CFRD by more than an order of magnitude compared to the next most significant variant (Supplemental Table 1; Figure 1A).

To determine whether any combination of physically close variants display more robust association with age-at-onset of CFRD than individual variants, we conducted burden testing using the SKAT-O algorithm on 5kb sliding windows (see Methods for details). For reference, 5kb was sufficiently large to encompass all genome-wide significant variants in the 5' region of *SLC26A9*. Numerous combinations of common variants (minor allele frequency; MAF>1%) in intron 1 and 5' of *SLC26A9* significantly associated with age-at-onset of CFRD (p<2.7E-4) but none achieved greater significance than observed with individual common variants in this region (Figure 1B, top panel). Notably, variant combinations that included rs7512462 in intron 5 generated less robust evidence of association than variant combinations in intron 1 and 5' of *SLC26A9*. None of the rare variants or 5kb windows containing only rare variants were significantly associated with age-at-onset of CFRD (Figure 1B, bottom panel). These results show that neither a single common or rare variant nor a combination of physically close variants solely accounts for the association with age-at-onset of CFRD in this region. Consequently, we tested the effects of association of the naturally occurring combinations of variants (i.e., haplotypes) with age-at-onset of diabetes.

CFRD-associated variants are in linkage disequilibrium and combine into haplotypes that associate with either high risk or low risk of CFRD. The analysis of single and small clusters of variants suggested that association with CFRD is likely due to multiple variants, possibly distributed over several regions of *SLC26A9*. To address this concept, we derived the haplotypes formed by common variants (MAF>15%) for all 762 individuals that were sequenced. Two ancestrally maintained regions (i.e., linkage disequilibrium (LD) blocks) defined by a single recombination event between introns 5 and 8 were identified (Figure 2A bottom; note *SLC26A9* is on the (-) DNA strand). All CFRD-associated variants located in the region encompassing portions of intron 5 and extending 9.9 kb 5' of the first exon of *SLC26A9* were commonly inherited together (i.e., high LD; D'>0.80) (Figure 2A bottom). This LD block has two common haplotypes that associated with CFRD; one associated with later onset of CFRD (Low Risk; LR; Minor

Haplotype Frequency (MHF): 28.4%; p-value: 1.14E-03) while the second associated with earlier onset of CFRD (High Risk; HR; MHF: 24.1%; p-value: 4.34E-03) (Figure 2A top). The LR haplotype contains all the alleles of the variants that associated with later onset of CFRD in the GWAS (8) (labeled with * in Supplemental Figure 1), and the HR haplotype contains all alleles associated with earlier onset of CFRD. The finding that the HR and LR haplotypes were associated with CFRD is based on 594 individuals with phenotype information available, of which 457 have at least one HR or LR haplotype and 137 did not. In addition to reporting the significance of the association of the LR and HR haplotypes with age-at-onset of CFRD, we illustrated the strength of the clinical association in the dataset by performing a log-rank test for difference in proportion with CFRD in the 82 individuals carrying either two copies of the LR haplotype or two copies of the HR haplotype. Using this subset of individuals, we show that the cumulative incidence of CFRD differed significantly between individuals homozygous for the LR haplotype (LR/LR) and those homozygous for the HR haplotype (HR/HR); log-rank p-value: 6.5E-3; Figure 2B). From a clinical perspective, by age 40, >80% of individuals with two copies of the HR haplotype (HR/HR) have developed CFRD compared to only ~25% of LR/LR individuals. A third less common haplotype (High Risk 2) that shares 11 of the 12 CFRD-associated alleles with the HR haplotype also associated with earlier age-at-onset of diabetes (Supplemental Figure 1). These analyses indicated that the *SLC26A9* variants operate in concert to modify age-at-onset of diabetes in CF.

***SLC26A9* mRNA transcripts from pancreas, lung and stomach contain non-coding exon 1**. Exon 1 of *SLC26A9* is predicted to be non-coding contributing only to the 5' untranslated sequence mRNA transcripts. As non-coding 5' exons can play a role in temporal or spatial gene expression (10), the location of the CFRD-associated variants upstream and downstream of exon 1 suggested that they may influence SLC26A9 expression. However, alternative splicing of the 5' end of *SLC26A9* leading to exclusion of exon 1 has been reported by the Human and Vertebrate Analysis and Annotation (HAVANA) project (http://www.sanger.ac.uk/research/projects/vertebrategenome/havana/). Furthermore, the transcription start site (TSS) of *SLC26A9* has only been mapped in RNA from human lung. Therefore, we sought to determine whether *SLC26A9* transcripts in additional tissues relevant to CF, contained non-coding exon 1 and if so, the exact location of the TSS using 5' Rapid Amplification of cDNA Ends (RACE). 5' RACE products from three unrelated human lung samples (5, 16, 8 transcripts, respectively), one human stomach sample (3 transcripts) and one human pancreas sample (2 transcripts) confirmed that *SLC26A9* mRNA transcripts contain exon 1 and that the TSS map in all three tissues to chr1:205,912,584 (hg19) (Figure 3). The major TSS is four nucleotides 3' relative to a previously reported TSS (10). The sequencing traces were contiguous across 4 exon-exon junctions confirming that amplification was from mRNA transcript. Four 5' RACE transcripts from one of the 3 lung samples had an alternative TSS beginning at position chr1:205,912,548 (hg19) which is 56 nucleotides upstream of the exon1/exon 2 junction. It is not clear if this is a minor TSS or the result of incomplete extension of the 5' RACE. The establishment of the TSS confirmed that the first exon of the *SLC26A9* gene is embedded within the variants that form the CFRD risk haplotypes.

Regulatory regions in the 5' region and first intron of *SLC26A9*. The region 5' of the major TSS contains a TATA (TATAAAC) box 29 bp upstream as well as a CCATT (GCCAATC) box 77 bp upstream. In addition, the region encompassing exon 1 and extending approximately 550 bp upstream is highly conserved across species (Figure 4). These features are attributes of a basal promoter. To search for potential regulatory regions encompassing exon 1 of *SLC26A9*, we used the Open Regulatory Annotation database (ORegAnno) track on the UCSC genome browser, which contains curated regulatory annotation derived from experimental data (41) (Figure 4). General binding sequences (GBSs) that interact with transcription factors (TFs) *GATA3, NFYA* and *NFYB* were mapped to the immediate 5' region (Figure 4, blue highlighted box). While the CFRD-associated variant rs1342063 falls within a TF cluster in this region, it does not affect any consensus TF binding motif according to the JASPAR core database (42). Also present 5' of exon 1 are GBSs that interact with *FOS, JUNB, JUND,* and *FOSL2* (Figure 4, yellow highlighted box) as well as for *MAFF, MAFK, TFAP2C, FOXA1, GATA3,* and *TFAP2A* (Figure 4, green highlighted box). In intron 1, GBSs that interact with *FOXA1, STAT1, SP1, USF2, TFAP2C and MAX* have been mapped. CFRD-associated variant rs7555534 in intron 1 falls within the GBS of *TFAP2C* and *FOXA1* but it does not alter any consensus binding motifs for the TFs according to the JASPAR core database (42). The location of ENCODE regulatory regions 5kb upstream of exon 1 and within the first intron suggests that CFRD risk haplotypes influence the expression of *SLC26A9*.

***SLC26A9* and *CFTR* are co-expressed in a discrete population of pancreatic cells with ductal characteristics.** To assess which pancreatic cell types express *SLC26A9*, and whether it is co-expressed with *CFTR*, we conducted single-cell RNA-sequencing (scRNA-seq) of the pancreas obtained from a pediatric individual with early chronic pancreatitis in the absence of CF. Using the Seurat pipeline (43), we were able to identify all major pancreatic cell types in addition to a cell type that contained characteristics of ductal and acinar cells (ductal/acinar; Figure 5A). Of the 2,999 of pancreatic single cells, *CFTR* was expressed in 531 cells (86.5% ductal and ductal/acinar), *SLC26A9* was expressed in 15 cells, and 11 cells expressed both *SLC26A9* and *CFTR* (100% ductal and ductal/acinar; hypergeometric test for co-expression p-value: 2.31E-07) (Figure 5B and C and Table 1). Re-analysis of scRNA-seq data from four studies containing a total of 31 pancreatic samples obtained from individuals of varying age and disease status (4 adults (44); 7 healthy adults, 1 T1D adult, 3 T2D adults, 2 healthy children (45); 4 adults (46) and 6 healthy and 4 T2D donors of varying BMI and age (47)) revealed that *CFTR* and *SLC26A9* are co-expressed in a small subset of ductal pancreatic cells in each dataset (Table 2). Data from two studies (44, 47) also confirmed that the co-expressing cells were primarily ductal (Figures 5D and E). The fraction of ductal cells that express CFTR ranges from 35.7% to 96.9% across studies. *SLC26A9* expression is detected in a lower fraction of ductal cells ranging from 1.4% to 17%. This variation likely reflects the different pancreatic tissue sampling approaches in the three studies, as illustrated by their differences in cellular composition (Supplemental Table 2). While *CFTR* is expressed at relatively high levels in a fraction of ductal cells, both *CFTR* and *SLC26A9* demonstrated variable expression among acinar and acinar/ductal cells in our sample (Supplemental Figure 2). It is important to mention that the co-expression of *CFTR* and *SLC26A9* is not merely due to the broad presence of *CFTR* in ductal cells and presence of *SLC26A9* in the same cell type. The hypergeometric test showed that the co-occurrence of both transcripts in the same cells is highly significant given the distribution of the two genes across all pancreatic cell types. Of note, *CFTR* RNA expression is very low in beta cells (2/531 CFTR-expressing cells are beta cells) while prominently transcribed in ductal cells (Table 2). This finding was consistent with our re-analysis of data from other studies (10/478 (47) and 0/389 (44) of *CFTR*-expressing cells are beta cells) (Figures 5D and E) and with re-analyses reported by other groups (48, 49).

We next determined whether pancreatic cells that express *SLC26A9* also express the TFs that have binding sites surrounding exon 1 (Figure 4). *FOS*, *JUNB* and *JUND* transcripts were broadly expressed and found in the majority of cells expressing *SLC26A9* (Table 1). At the other end of the spectrum, *FOXA1, TFAP2C, GATA3* and *TFAP2A* transcripts were not detected in cells expressing *SLC26A9* in our pancreatic sample. Of the TFs expressed in fewer cells (32 to 296 out of 2999 cells), *FOSL2, SP1*, and *MAFK* are co-expressed in a small but significant fraction of *SLC26A9*-expressing cells (Table 1; above dotted line). Re-analysis of four published pancreatic scRNA-seq datasets (44-47) revealed similar patterns with *FOS*, *JUNB* and *JUND* being broadly expressed and found in the majority of *SLC26A9*-expressing ductal cells while *FOSL2* and *SP1* were expressed in fewer cells but significantly co-expressed with *SLC26A9* (Table 2) (44-47). Furthermore, *FOXA1, TFAP2C, GATA3* and *TFAP2A* TFs were either absent or present in only a few cells that expressed *SLC26A9.* One notable difference from our scRNA-seq data was that *MAFF* was present in a relatively high fraction of *SLC26A9*-expressing cells in all four published datasets. From these results, we noted that binding sequences of the four TFs consistently present in *SLC26A9*-expressing cells (*FOS, JUNB, JUND* and *FOSL2*) occur in a cluster 5' of exon 1 (Figure 4).

To characterize the pancreatic ductal cells that express *SLC26A9*, we evaluated expression of apical and/or basolateral channels and bicarbonate transporters using our scRNA-seq data and the four publicly available data sets. We focused our search on genes encoding proteins that have been detected in pancreatic ductal cells by biochemical and electrophysiological methods (50-52). We also examined the expression of selected genes relevant to *SLC26A9* and *CFTR* (e.g. WNK family and *FOXI1+*). Our analysis revealed that cells expressing *CFTR* and *SLC26A9* also consistently express Aquaporin 1 (*AQP1*) and *SLC4A4* (*NBCe1-B*) in our scRNA-seq study and the four publicly available datasets (Supplemental Table 3). In most studies, *SCNN1A* (*ENaC* alpha subunit), *SLC4A2* (*AE2*) and activators (*STK39* (*SPAK*) and *WNK1*) appear to be expressed in ductal cells that co-express *SLC26A9* and *CFTR*. Notably absent (or very minimally expressed) are *WNK4* and other SLC26 transporters (A3, A4 and A6). We did not find evidence of a cell population that expressed high levels of *CFTR* along with FOXI1+ or vATPase genes *(ATP6V1C2* and *ATP6V0D2*) similar to ionocytes that have been reported in the lung (53, 54)**.**

DNA fragments 5' of *SLC26A9* bearing CFRD low risk haplotype generate higher levels of reporter gene expression than high risk CFRD haplotype. To determine if the region containing the diabetes-associated variants drive expression at different levels in the pancreas, four DNA fragments from the 5' region of *SLC26A9* (Figure 6A) containing either HR and LR variants were cloned into a firefly luciferase reporter construct (pGL4.10, Promega) in the native orientation (*SLC26A9* resides on the negative strand). All *SLC26A9* constructs were tested in the PANC-1 cell line, a human pancreatic adenocarcinoma cell line that is of ductal cell origin (55) but also is a surrogate for pancreatic progenitor cells since they can be induced to differentiate into insulin-producing cells (56). A renilla construct (pRL-TK, Promega) was included to normalize for transfection efficiency. Analysis of RNA-seq data available on the sequence read archive demonstrated that PANC-1 cells express TFs *FOS, JUNB, JUND* and *FOSL2* that have putative binding sites in the 5' region of *SLC26A9* (Table 1). Both *SLC26A9* and *CFTR* are expressed in PANC-1 cells, albeit at low levels relative to the aforementioned TFs (Table 1) likely due to inactivation of their promoters, as observed in other immortalized cell lines (57).

The 1.172 kb DNA fragment immediately adjacent to exon 1 generated robust luciferase expression consistent with our expectation that this region encompassed the basal promoter of *SLC26A9*. Although 2 CFRD-associated variants are in this region, no differences in expression levels were noted when DNA fragments bearing the LR (blue) or HR (red) alleles were analyzed (Figure 6B). We next examined the region immediately adjacent and upstream of the 1.172 kb region that contains 3 CFRD-associated variants. Constructs containing the 1.173kb region displayed little to no luciferase expression, similar to negative controls (Figure 6B). However, when fused to the 1.172 kb region to form a contiguous 2.3 kb fragment, we noted that 3 out of the 4 LR 2.3kb clones consistently differed in luciferase expression levels from clones with HR alleles (Figure 6B). Combined analysis of the normalized data from 3 independent transfections with 4 biological clones per haplotype (technical replicates: transfection well N=71 for LR and N=72 for HR; Supplemental Figure 3) revealed that the fragment containing variants associated with LR of diabetes had a difference in means of 12% higher activity compared to HR (p-value: 5.15E-09). Addition of 2.5 kb of sequence from the region immediately adjacent and upstream of the 2.3 kb regions formed a 4.8 kb fragment containing all 6 of the CFRD-associated variants residing 5' of *SLC26A9.* Notably, both clones bearing the LR haplotype generated an overall difference in means of 19% higher expression level compared to clones bearing the HR haplotype (p-value: 6.28E-07) (Figure 6B).

We also tested the 2.3 kb LR and HR constructs in a second cell line, CFPAC-1, a pancreatic ductal adenocarcinoma cell line derived from an individual with CF (58, 59). CFPAC-1 cells express TFs *FOS, JUNB, JUND* and *FOSL2* and have very low levels of endogenous *CFTR* and *SLC26A9* expression, as noted for PANC-1 cells (Table 1). LR constructs demonstrated significantly higher expression than HR constructs in two independent transfections of 4 clones per construct (Figure 6C). Overall, LR exhibited 20% higher expression than HR (p-value: 2.00E-03 (N=48 for LR, N=47 for HR)) in CFPAC-1 cells. From these results, we concluded that CFRD-associated variants in the

5’ region act in concert with its basal promoter to alter the expression of *SLC26A9* in pancreatic cells.

eQTL analysis suggests that low risk alleles of CFRD variants are associated with increased expression of *SLC26A9*. We downloaded publicly available data from the Genotype-Tissue Expression (GTEx, v7) portal to determine whether the CFRD risk variants associate with *SLC26A9* RNA expression in the pancreas. Results show that the CFRD-associated variants associate with *SLC26A9* RNA expression in the pancreas. Alleles on the LR haplotype were associated with increased expression of *SLC26A9* in the pancreas, but it did not correlate with expression in the lung (Supplemental Table 4), as recently reported (31).

Discussion

The goal of this study was to determine if variants associated with age-at-onset of cystic fibrosis-related diabetes (CFRD) affected the expression of *SLC26A9*. We discovered that the alleles of the CFRD-risk variants are co-inherited as two common haplotypes, one that is associated with later onset of CFRD (Low Risk; LR), and the other that is associated with earlier onset of CFRD (High Risk; HR). A third less common haplotype similar to HR also associated with earlier onset of diabetes and it is possible that other less common haplotypes bearing the majority of the CFRD-risk variants also correlate with CFRD, but are not sufficiently frequent to allow detection of association in the 762 individuals studied here. There was no evidence that a coding or rare variant accounted for the CFRD association. Mapping of the major TSS indicate that the non-coding first exon of *SLC26A9* is placed in the middle of the cluster of CFRD-risk variants in the 5' region of *SLC26A9*. These results suggested that the HR and LR CFRD haplotypes affect transcriptional regulation of *SLC26A9*. Characterization of the transcription factor binding sites 5' of exon 1 and profiling of the transcriptome of the ductal pancreatic cells that express *SLC26A9* indicated that the TFs *FOS* and *JUN* likely direct *SLC26A9* expression. DNA fragments derived from the 5' region of *SLC26A9* were transcriptionally active in pancreatic ductal cell line models (PANC-1 and CFPAC-1) that express *FOS* and *JUN* TFs. Reporter assays showed that the presence of variants corresponding to the LR haplotype showed 12-20% higher levels of expression compared to the HR haplotype in both pancreatic ductal cell lines. The CFPAC-1 cell line demonstrated that absence of *CFTR* (as seen in CF) did not alter the difference in expression between the LR and HR constructs. Collectively, our findings indicate an increase in the expression of *SLC26A9* in ductal cells of the pancreas delays the age-at-onset of diabetes in individuals with CF.

Locating the 5’ TSS was essential to establish whether the non-coding exon 1 was included in *SLC26A9* RNA transcripts. Mapping to the same nucleotide in multiple independent transcripts from three different tissues (pancreas, lung and stomach) confirmed that the full-length transcript had been obtained. As the previously reported TSS was also determined using RNA from the lung, the inconsistency between the major TSS we found and the previously reported TSS (4 base pairs longer (10) is likely due to technical reasons. Placement of the TSS upstream of exon 2 verifies inclusion of a non-coding first exon in the majority of *SLC26A9* transcripts. Non-coding first exons have been generally thought to fulfill regulatory roles in gene expression (e.g. by controlling translation efficiency and mRNA stability). This control may occur through the primary sequence of the 5’UTR as well as secondary structure of the RNA. The latter governs the recognition and interaction with a combination of factors important for translation and stability (60, 61). However, we did not discover any variants in the 5’UTR of *SLC26A9* encoded by exon 1 that might be postulated to affect transcript stability, leading us to focus on upstream sequences.

To assess the appropriate cellular context for evaluating the putative regulatory regions and the effect of the CFRD-associated variants, we established the pancreatic cell types that express *SLC26A9*. Single-cell RNA-sequencing (scRNA-seq) revealed that *SLC26A9* is expressed in a minor fraction of ductal cells. Since our study was performed on a single pediatric chronic pancreatitis case, we confirmed and extended our findings using scRNA-seq data from four additional publicly available studies of 31 pancreas tissues from children and adults (44-47). We have not been able to evaluate the expression profile of *SLC26A9* during development when exocrine pancreatic damage first occurs in individuals with CF. This is likely to be relevant as observations in mice indicate that *SLC26A9* expression is considerably higher in utero and decreases shortly after birth (22). Notably, *CFTR* is present in the majority of the pancreatic cells that express *SLC26A9* and 100% of the cells expressing both genes are ductal or ductal/acinar. Evidence of co-expression supports the concept that SLC26A9 and CFTR interact in vivo, as suggested by in vitro and cell-based studies (13, 19, 62). We have further evaluated the expression level of key genes in the WNK pathway whose proteins regulate SLC26A9 activity. Among the five scRNA-seq studies, there was evidence of *WNK1* and *STK39* (*SPAK*) being expressed in cells with *SLC26A9* while *WNK4* was almost absent.

How could variation in *SLC26A9* expression in a small subset of ductal cells affect risk for diabetes in CF? First, it has been shown that transcript copy number correlates modestly with protein concentration (63). Thus, *SLC26A9* protein levels might be considerably higher in ductal cells than the levels implied by counts of RNA transcript. Second, it is possible that the *SLC26A9* expressing cells play a critical role in ductal ion transport, perhaps by being anatomically clustered in one portion of the pancreatic duct. This situation might be analogous to ionocytes in the lung, a rare cell type that expresses high levels of *CFTR* (53, 54). We did not, however, consistently observe expression of FOXI1+ or vATPase genes *(ATP6V1C2* and *ATP6V0D2*) that characterize ionocytes in the *SLC26A9/CFTR* co-expressed pancreatic cells (Supplemental Table 3). Third, the cells that express *SLC26A9* may have other key roles in the pancreas, such as that reported for centroacinar cells (CACs), a specialized ductal cell-type found near acini that express CFTR in fetal and adult pancreas (64, 65) that can replenish beta cells in zebrafish and mammals (64, 66, 67).

Though the etiology of CFRD is incompletely understood and is likely multifactorial, it has been documented that insulin secretion diminishes as individuals with CF age due to inflammation and destruction of pancreatic islet cells (49). Other studies report that CFTR plays a direct role in the release of insulin and glucagon as well as in the protection of beta cells from oxidative stress and in controlling the resting potential of alpha and beta cells in rats (68). CFTR has also been proposed as a glucose-sensing negative regulator of glucagon secretion in alpha cells in mice, a defect postulated to contribute to glucose intolerance in CF and other forms of diabetes (69). However, several observations question whether CFTR plays a direct role in insulin release from beta cells (36, 38, 40, 44, 47-49, 70, 71). Whether loss of CFTR function in beta cells does or does not contribute to the development of diabetes in CF, there is growing evidence that variation in the risk of CFRD correlates with ductal (i.e., exocrine) dysfunction. For example, the CFRD-associated variant rs7512462 in intron 5 of *SLC26A9* has been associated with variation in newborn immunoreactive trypsinogen levels, a biomarker of prenatal exocrine pancreatic disease (29). Of note, exocrine pancreatic dysfunction has been observed in 10-30% of individuals with T1D and T2D

(72, 73). Furthermore, loss of function of the pancreatic enzyme carboxyl ester lipase due to deleterious genetic variants were associated with exocrine pancreatic disease and diabetes in two families (74). Together, these studies support the concept that aberrant exocrine ductal function can be a major contributor to reduced insulin secretion and the development of diabetes.

Based on crowd-sourced assessments provided in the Open Regulatory Annotation database, we suspected that the cluster of transcription factor binding sites for *FOS, JUNB*, *JUND*, and *FOSL2* act as enhancers for *SLC26A9* expression. This assertion was supported by the observation that the DNA fragment containing these putative binding sites drives expression only when fused to the native *SLC26A9* promoter (2.3kb fragment). Members of the *FOS* and *JUN* family are well known to dimerize via leucine zippers to create the AP-1 TF complex (75). AP-1 activity has been implicated in a variety of normal cellular function such as proliferation, differentiation and apoptosis as well as abnormal processes, in particular, neoplastic transformation (76). Thus, the expression of *FOS* and *JUN* in a cancer cell line such as the pancreatic adenocarcinoma (PANC-1) cell line used in our studies is expected. However, we posit that these TFs have a physiologic role in *SLC26A9* expression as RNA encoding these TFs are consistently expressed in the subset of ductal cells that express *SLC26A9* (44-46). Furthermore, we observed that the *SLC26A9* 2.3 kb construct expressed in the CFPAC-1 cells, a pancreatic adenocarcinoma cell line derived from an individual with CF (58, 59). *FOS* TFs have been implicated in diabetes and glucose homeostasis. Computational analysis has suggested that *FOS* plays a role in the pathogenesis of

T2D (77) and *FOSL2* in T2D individuals has been shown to be hypermethylated leading to lower mRNA and protein expression levels (78). Finally, we observed that TFs *FOXA1*, *TFAP2A* and *2C* and *GATA3* that are known to be associated with type 2 diabetes risk (79), development and subsequent maintenance of beta cells (80) and insulin secretion (81) were absent in *SLC26A9*-expressing pancreatic cells in our study and in two of the four published studies (44, 45). The absence of these TFs likely explains why the 4.8kb fragment containing the 2.5 kb region (that has binding sites for *FOXA1*, *TFAP2A* and *2C* and *GATA3*) displayed a similar level of reporter expression and maintained the allele-dependent expression observed with the 2.3 kb fragment. Together, these findings support a role for FOS and JUN in the transcriptional regulation of *SLC26A9* in the post-natal pancreas.

Age-at-onset of diabetes in CF is a complex trait modified by multiple genes that develops over the lifetime of individuals with CF (8). As such, the ~20% difference between the expression level of LR and HR haplotypes in PANC-1 and CFPAC-1 cells is consistent with the modest effect size attributable to a gene operating in the context of a complex disorder (35, 82). Indeed, more substantial changes in *SLC26A9* expression cause distinct intestinal and pulmonary phenotypes in knock-out mouse models (17, 20). Although we have not yet been able to determine the precise element(s) that is responsible for the difference observed between LR and HR haplotypes, this information is not essential for moving forward with a strategy to treat CFRD. There is growing evidence that provision of alternative pathways for chloride transport via channels such as TMEM16A (83) or small molecule ion channels (84) can restore anion secretion in CF tissues. Likewise, several studies suggest that SLC26A9, a chloride/bicarbonate transporter may be able to compensate for the loss of CFTR function in individuals with CF (15, 85, 86). Consequently, our results indicate that strategies that increase the level and/or function of SLC26A9 provide a viable approach to delaying the onset of diabetes in CF.

Material and Methods

Diagnosis of CFRD

The CFRD phenotype was defined using data extracted from medical charts or CFF Patient Registry. Minimum criteria include clinical diagnosis of CFRD and at least 1 year insulin use (9). Supporting lab data was used when available including glucose tolerance and hemoglobin A1c (the HbA1c is not used to rule out diabetes but can be used to rule it in; as per CFRD guidelines). Fasting glucose was found to have low specificity for CFRD after review of chart data and was not used in the definition of CFRD.

Resequencing Cohort and Capture

A total of 762 p.Phe508del homozygotes recruited as a part of the Johns Hopkins Twin and Sibling Study (TSS) and University of North Carolina's Genetic Modifiers Study (GMS) were analyzed. Cohort selection, sample consent and DNA preparations were previously described (87). A total of 47.7kb encompassing *SLC26A9* and extending 9.9kb 5' and 7.4kb 3' of the gene were deep sequenced (Capture design, library prep, sequencing, variant call and annotation and data cleaning as reported by Vecchio-Pagán *et al., 2016* (87))**.**

Linkage Disequilibrium, Haplotype Block Analysis and Association Testing

Each variant was associated with the martingale residual phenotype for cystic fibrosis-related diabetes (CFRD) using a linear regression in the PLINK software package v1.07 (88). Data was initially cleaned for individual and variant missingness and IBD structure to remove related samples. Individual variants association with CFRD was conducted using --assoc command on PLINK. Log transformed p-values were plotted as a locus zoom plot using LocusZoom (89) in Figure 1A. For haplotype-based association testing, the analysis was conducted in PLINK using the --chap and --each-vs-others commands. Only haplotypes with frequencies >2% containing variants with frequencies >15% were derived. LD blocks and haplotypes were confirmed and visualized using Haploview (Figure 2; Supplemental Figure 1).

Common and Rare Variant Burden Testing

To check for association between sets of variants and CFRD, a 5kb sliding window was moved across the entire 47.7kb capture region in 1250bp increments, and common and rare variants (MAF cut-off: 1% in our population) falling within these regions were grouped for region-based burden testing using the SKAT-O algorithm (90). In the 47.7kb captured region encompassing the *SLC26A9* locus and surrounding genes, a total of 36 windows were present. The SKAT-O algorithm was implemented in R, using the “SSD” commands which allow for loading of a plink formatted dataset, and the “optimal.adj” method, representing the optimized method.

Determination of transcription start site of *SLC26A9*

5’ Rapid Amplification of cDNA Ends (RACE) was performed using the SMARTer (“Switching Mechanism At RNA Termini”) RACE cDNA Amplification Kit (Clontech). RNA isolated from primary tissue (pancreas, lung and stomach) obtained from the Johns Hopkins Pathology Department was used to synthesize the first-strand cDNA and

5’-RACE-Ready cDNA with the SeqAmp^{TM} DNA Polymerase in accordance with the manufacturer’s instructions. The gene-specific primer (5’GATTACGCCAAGCTTGGCAGGCTAGCGTAGCTGACACG-3’) sitting in exon 5 of *SLC26A9* was used for RACE PCR and the products containing the 15 bp overlap (GATTACGCCAAGCTT) were cloned into the linearized pRACE vector with In-Fusion® HD Cloning. Plasmids were sent for Sanger sequencing with M13F and M13R primers.

Single-cell RNA-sequencing of pancreatic cells

Preparation of single cells and processing of RNA-Seq reads: Supplemental Section. Following processing of RNA-Seq reads, a total of 2,999 cells and 16,884 genes were retained. Gene counts were log-normalized following filtering of the gene-barcode matrix. Seurat was used to identify highly variable genes (default parameters, except dispersion selection method), perform principal component analysis (with n=1000 highly variable genes), and determine significant principal components. The t-SNE projection was generated with the first 12 principal components. Graph-based clustering with K-nearest neighbor was used to predict cell populations. Cell specific expression markers identified from previous single cell papers (46) were then used to define and divide predicted clusters–acinar (*PRSS1, PNLIP*), beta (*INS*), alpha (*GCG*), delta (*SST*), PP (*PPY*), ductal (*KRT19*, *SPP1, ATP1B, SLC4A4*), endothelial (*ESAM*), mesenchyme (*THY1, COL1A1*).

Reanalysis of published single-cell RNA-Sequencing of the Pancreas

Single-cell RNA-sequencing of the pancreas conducted by the studies referenced in Table 2 were reanalyzed. Data was downloaded from the gene expression omnibus repository (accession numbers GSE84133, GSE83139, GSE85241) and the ArrayExpress (EBI) (E-MTAB-5061), and analyzed in R. Significance of co-expression was determined with a hypergeometric test, using the phyper function (phyper(# of cells co-expressing *SLC26A9* and gene B, number of cells expressing *SLC26A9*, # of cells that don't express *SLC26A9*, # of cells expressing *CFTR*)). Expression of a gene was defined by having a gene count >1 for data downloaded from the gene expression omnibus repository, and a log-normalized gene count >0.5 for our data.

Reanalysis of publicly available RNA-Sequencing data of PANC-1 and CFPAC-1 cells

RNA-sequencing data available in the sequence read archive were used (accession IDs SRR5171012, SRR5171013, SRR1172002, SRR3615309, SRR5952226; CFPAC-1: SRR1736491). Raw reads were aligned to the reference genome (hg19) using the Bowtie2 algorithm (91) and splice junctions were identified via Tophat2 (v2.0.13) (92) from the Tuxedo software suite. CuffQuant and Cuffdiff (Cufflinks v2.2.1) (93) were then used to assemble transcripts, estimate their abundances, and test for differential expression among samples.

Mammalian cell culture, transfection and Dual Luciferase-Renilla Reporter Assay

PANC-1 cells were maintained in Dulbecco's modified Eagle's medium (DMEM, Invitrogen) supplemented with 10% v/v fetal bovine serum (FBS) and 1% Penicillin-

Steptomycin (PS). CFPAC-1 cells were maintained in Iscover’s modified Dulbecco’s medium (IMDM, ThermoFisher Scientific) also supplemented with 10% v/v FBS and 1% PS. When PANC-1s/CFPAC-1s were approaching 70%-80% confluency, they were transfected with LR or HR reporter plasmids (Supplemental Figure 2) with Lipofectamine 2000 (Invitrogen) according to the manufacturer’s instructions and then placed in antibiotic free medium/FBS for 48 hours. As transfection and expression efficiency can vary due to the structure of the plasmids (e.g. coiled, supercoiled), we used up to 4 independently derived plasmid clones for each *SLC26A9* DNA fragment tested. A spectrophotometer was used to quantify DNA concentration. The number of plasmids used was calculated based on the concentration of the plasmid adjusted for size (molecular molar mass) thus, all transfections contain equal number of plasmid copies per technical replicate/well in each independent transfection (1.7E-13 mol or ~1.0E11 copies). To address biological variation, transfections were performed in 6-wells for at least 2-3 independent transfections per construct. As a control for the normalization of transfection efficiency, same amount of the renilla luciferase encoding plasmid pRL-TK (3.4E-15 mol or approximately 2.0E9 copies), is added to all transfection wells (94, 95). The neutral constitutive expression of *Renilla* luciferase was used as an internal control value to which expression of the experimental firefly luciferase reporter gene was normalized. Whole cell lysates were harvested after 15-minute incubation with 1x passive lysis buffer (Promega). All samples were centrifuged at maximum speed for 15 minutes at 4^{o}C and plated onto a 96-well plate in triplicates with 20 uL lysate per well then analyzed using the Dual-Luciferase® Reporter Assay System (Promega) on a BioTek plate reader (BioTek Instruments, Inc.). The luminometer was set to inject 50 uL of Luciferase Assay Buffer II (LARII) and 50 uL Stop & Glo Reagent sequentially into each sample for independent measurement of fLUC and rLUC activities. Each injection was followed by slow shake for 3 seconds followed by an integration period allotted by a 2 seconds delay. Luminescence for both fLUC and rLUC, and the relative ratio of fLUC/rLUC activity was recorded in an excel file.

Study approval

Samples were obtained under approved research protocols from Johns Hopkins Pathology Department (IRB00157289, Date of Acknowledgement is 8/16/2018. Date of Expiration is 8/16/2021) and the University of Pittsburgh (IRB# PRO16030614 for demographic information and PRO13020493 for genetic evaluation of pancreatic surgical waste).

Author Contributions

ANL performed data analysis, designed and performed experiments, contributed to data interpretation and wrote the manuscript. MAA performed data analysis and assisted in writing the manuscript. BVP performed data analysis. AFA assisted in the plasmid construction. LAG assisted in data interpretation. CAS and DOL performed experiments. DCW contributed to experimental design. SMB contributed to the overall design of project, data analysis and manuscript writing. GRC directed the overall research, experimental design, data interpretation and wrote the manuscript.

Acknowledgements

The authors thank Dr. Michael Knowles and Rhonda Pace for providing samples for the resequencing study and Dr. Jun Shen for her technical support during the early phase of the project. We thank all of the HAVANA team that contributed to the manual annotation. Additionally, we thank the Genotype-Tissue Expression (GTEx) Project, which was supported by the Common Fund of the Office of the Director of the NIH, and by NCI, NHGRI, NHLBI, NIDA, NIMH, and NINDS. The data used for the analyses described in this manuscript were obtained from: gtexportal.org on 03/08/19. This work was supported in part by the United States Cystic Fibrosis Foundation (CFF) (CUTTIN13A2, CUTTIN17G0) and by the NIH (DK44003) for GRC, CFF (BLACKM16G0, BLACKM16A0), and Gilead Sciences for SMB. ANL was supported in part by training grant T32GM07814. LAG is supported by the NSF (IOS-1656592), the Maryland Stem Cell Research Fund (2016-MSCRFI-2805), the Chan-Zuckerberg Initiative DAF (2018-183445), and the Johns Hopkins University Catalyst and Synergy Awards. This research was partly supported by NIH grants U01 DK108306, DK098560 to DCW, and DK063922 to CAS.

1. Davies JC, Alton EW, and Bush A. Cystic fibrosis. *BMJ.* 2007;335(7632):1255-9.
2. Foundation CF. Cystic Fibrosis Foundation Patient Registry Annual Data Report 2017.
3. Moran A, Brunzell C, Cohen RC, Katz M, Marshall BC, Onady G, et al. Clinical care guidelines for cystic fibrosis-related diabetes: a position statement of the American Diabetes Association and a clinical practice guideline of the Cystic Fibrosis Foundation, endorsed by the Pediatric Endocrine Society. *Diabetes Care.* 2010;33(12):2697-708.
4. Lewis C, Blackman SM, Nelson A, Oberdorfer E, Wells D, Dunitz J, et al. Diabetes-related mortality in adults with cystic fibrosis. Role of genotype and sex. *Am J Respir Crit Care Med.* 2015;191(2):194-200.
5. Milla CE, Warwick WJ, and Moran A. Trends in pulmonary function in patients with cystic fibrosis correlate with the degree of glucose intolerance at baseline. *Am J Respir Crit Care Med.* 2000;162(3 Pt 1):891-5.
6. Gottlieb PA, Yu L, Babu S, Wenzlau J, Bellin M, Frohnert BI, et al. No relation between cystic fibrosis-related diabetes and type 1 diabetes autoimmunity. *Diabetes Care.* 2012;35(8):e57.
7. Couce M, O'Brien TD, Moran A, Roche PC, and Butler PC. Diabetes mellitus in cystic fibrosis is characterized by islet amyloidosis. *J Clin Endocrinol Metab.* 1996;81(3):1267-72.
8. Blackman SM, Commander CW, Watson C, Arcara KM, Strug LJ, Stonebraker JR, et al. Genetic modifiers of cystic fibrosis-related diabetes. *Diabetes.* 2013;62(10):3627-35.
9. Blackman SM, Hsu S, Vanscoy LL, Collaco JM, Ritter SE, Naughton K, et al. Genetic modifiers play a substantial role in diabetes complicating cystic fibrosis. *J Clin Endocrinol Metab.* 2009;94(4):1302-9.
10. Lohi H, Kujala M, Makela S, Lehtonen E, Kestila M, Saarialho-Kere U, et al. Functional characterization of three novel tissue-specific anion exchangers SLC26A7, -A8, and -A9. *J Biol Chem.* 2002;277(16):14246-54.
11. Dorwart MR, Shcheynikov N, Wang Y, Stippec S, and Muallem S. SLC26A9 is a Cl(-) channel regulated by the WNK kinases. *J Physiol.* 2007;584(Pt 1):333-45.
12. Loriol C, Dulong S, Avella M, Gabillat N, Boulukos K, Borgese F, et al. Characterization of SLC26A9, facilitation of Cl(-) transport by bicarbonate. *Cell Physiol Biochem.* 2008;22(1-4):15-30.
13. Chang MH, Plata C, Sindic A, Ranatunga WK, Chen AP, Zandi-Nejad K, et al. Slc26a9 is inhibited by the R-region of the cystic fibrosis transmembrane conductance regulator via the STAS domain. *J Biol Chem.* 2009;284(41):28306-18.
14. Salomon JJ, Spahn S, Wang X, Füllekrug J, Bertrand CA, and Mall MA. Generation and functional characterization of epithelial cells with stable expression of SLC26A9 Cl- channels. *Am J Physiol Lung Cell Mol Physiol.* 2016;310(7):L593-602.
15. Walter JD, Sawicka M, and Dutzler R. Cryo-EM structures and functional characterization of murine Slc26a9 reveal mechanism of uncoupled chloride transport. *Elife.* 2019;8.

16. Xu J, Song P, Miller ML, Borgese F, Barone S, Riederer B, et al. Deletion of the chloride transporter Slc26a9 causes loss of tubulovesicles in parietal cells and impairs acid secretion in the stomach. *Proc Natl Acad Sci U S A.* 2008;105(46):17955-60.

17. Liu X, Li T, Riederer B, Lenzen H, Ludolph L, Yeruva S, et al. Loss of Slc26a9 anion transporter alters intestinal electrolyte and HCO3(-) transport and reduces survival in CFTR-deficient mice. *Pflugers Arch.* 2015;467(6):1261-75.

18. Amlal H, Xu J, Barone S, Zahedi K, and Soleimani M. The chloride channel/transporter Slc26a9 regulates the systemic arterial pressure and renal chloride excretion. *J Mol Med (Berl).* 2013;91(5):561-72.

19. Bertrand CA, Zhang R, Pilewski JM, and Frizzell RA. SLC26A9 is a constitutively active, CFTR-regulated anion conductance in human bronchial epithelia. *J Gen Physiol.* 2009;133(4):421-38.

20. Anagnostopoulou P, Riederer B, Duerr J, Michel S, Binia A, Agrawal R, et al. SLC26A9-mediated chloride secretion prevents mucus obstruction in airway inflammation. *J Clin Invest.* 2012;122(10):3629-34.

21. Bakouh N, Bienvenu T, Thomas A, Ehrenfeld J, Liote H, Roussel D, et al. Characterization of SLC26A9 in patients with CF-like lung disease. *Hum Mutat.* 2013;34(10):1404-14.

22. Strug LJ, Gonska T, He G, Keenan K, Ip W, Boëlle PY, et al. Cystic fibrosis gene modifier SLC26A9 modulates airway response to CFTR-directed therapeutics. *Hum Mol Genet.* 2016;25(20):4590-600.

23. Kmit A, Marson FAL, Pereira SV, Vinagre AM, Leite GS, Servidoni MF, et al. Extent of rescue of F508del-CFTR function by VX-809 and VX-770 in human nasal epithelial cells correlates with SNP rs7512462 in SLC26A9 gene in F508del/F508del Cystic Fibrosis patients. *Biochim Biophys Acta Mol Basis Dis.* 2019;1865(6):1323-31.

24. Consortium G. The Genotype-Tissue Expression (GTEx) project. *Nat Genet.* 2013;45(6):580-5.

25. Xu J, Henriksnäs J, Barone S, Witte D, Shull GE, Forte JG, et al. SLC26A9 is expressed in gastric surface epithelial cells, mediates Cl-/HCO3- exchange, and is inhibited by NH4+. *Am J Physiol Cell Physiol.* 2005;289(2):C493-505.

26. Lee HJ, Yoo JE, Namkung W, Cho HJ, Kim K, Kang JW, et al. Thick airway surface liquid volume and weak mucin expression in pendrin-deficient human airway epithelia. *Physiol Rep.* 2015;3(8).

27. El Khouri E, and Touré A. Functional interaction of the cystic fibrosis transmembrane conductance regulator with members of the SLC26 family of anion transporters (SLC26A8 and SLC26A9): physiological and pathophysiological relevance. *Int J Biochem Cell Biol.* 2014;52:58-67.

28. Ousingsawat J, Schreiber R, and Kunzelmann K. Differential contribution of SLC26A9 to Cl(-) conductance in polarized and non-polarized epithelial cells. *J Cell Physiol.* 2012;227(6):2323-9.

29. Miller MR, Soave D, Li W, Gong J, Pace RG, Boëlle PY, et al. Variants in Solute Carrier SLC26A9 Modify Prenatal Exocrine Pancreatic Damage in Cystic Fibrosis. *J Pediatr.* 2015;166(5):1152-7.e6.

30. Soave D, Miller MR, Keenan K, Li W, Gong J, Ip W, et al. Evidence for a causal relationship between early exocrine pancreatic disease and cystic fibrosis-related diabetes: a Mendelian randomization study. *Diabetes.* 2014;63(6):2114-9.

31. Gong J, Wang F, Xiao B, Panjwani N, Lin F, Keenan K, et al. Genetic association and transcriptome integration identify contributing genes and tissues at cystic fibrosis modifier loci. *PLoS Genet.* 2019;15(2):e1008007.

32. Sun L, Rommens JM, Corvol H, Li W, Li X, Chiang TA, et al. Multiple apical plasma membrane constituents are associated with susceptibility to meconium ileus in individuals with cystic fibrosis. *Nat Genet.* 2012;44(5):562-9.

33. Blackman SM, Deering-Brose R, McWilliams R, Naughton K, Coleman B, Lai T, et al. Relative contribution of genetic and nongenetic modifiers to intestinal obstruction in cystic fibrosis. *Gastroenterology.* 2006;131(4):1030-9.

34. Kemaladewi DU, Bassi PS, Erwood S, Al-Basha D, Gawlik KI, Lindsay K, et al. A mutation-independent approach for muscular dystrophy via upregulation of a modifier gene. *Nature.* 2019;572(7767):125-30.

35. O'Neal WK, and Knowles MR. Cystic Fibrosis Disease Modifiers: Complex Genetics Defines the Phenotypic Diversity in a Monogenic Disease. *Annu Rev Genomics Hum Genet.* 2018;19:201-22.

36. Bellin MD, Laguna T, Leschyshyn J, Regelmann W, Dunitz J, Billings J, et al. Insulin secretion improves in cystic fibrosis following ivacaftor correction of CFTR: a small pilot study. *Pediatr Diabetes.* 2013;14(6):417-21.

37. Tsabari R, Elyashar HI, Cymberknowh MC, Breuer O, Armoni S, Livnat G, et al. CFTR potentiator therapy ameliorates impaired insulin secretion in CF patients with a gating mutation. *J Cyst Fibros.* 2016;15(3):e25-7.

38. Thomassen JC, Mueller MI, Alejandre Alcazar MA, Rietschel E, and van Koningsbruggen-Rietschel S. Effect of Lumacaftor/Ivacaftor on glucose metabolism and insulin secretion in Phe508del homozygous cystic fibrosis patients. *J Cyst Fibros.* 2018;17(2):271-5.

39. Li A, Vigers T, Pyle L, Zemanick E, Nadeau K, Sagel SD, et al. Continuous glucose monitoring in youth with cystic fibrosis treated with lumacaftor-ivacaftor. *J Cyst Fibros.* 2019;18(1):144-9.

40. Kelly A, De Leon DD, Sheikh S, Camburn D, Kubrak C, Peleckis AJ, et al. Islet Hormone and Incretin Secretion in Cystic Fibrosis after Four Months of Ivacaftor Therapy. *Am J Respir Crit Care Med.* 2019;199(3):342-51.

41. Lesurf R, Cotto KC, Wang G, Griffith M, Kasaian K, Jones SJ, et al. ORegAnno 3.0: a community-driven resource for curated regulatory annotation. *Nucleic Acids Res.* 2016;44(D1):D126-32.

42. Mathelier A, Zhao X, Zhang AW, Parcy F, Worsley-Hunt R, Arenillas DJ, et al. JASPAR 2014: an extensively expanded and updated open-access database of transcription factor binding profiles. *Nucleic Acids Res.* 2014;42(Database issue):D142-7.

43. Butler A, Hoffman P, Smibert P, Papalexi E, and Satija R. Integrating single-cell transcriptomic data across different conditions, technologies, and species. *Nat Biotechnol.* 2018;36(5):411-20.

44. Baron M, Veres A, Wolock SL, Faust AL, Gaujoux R, Vetere A, et al. A Single-Cell Transcriptomic Map of the Human and Mouse Pancreas Reveals Inter- and Intra-cell Population Structure. *Cell Syst.* 2016;3(4):346-60.e4.

45. Wang YJ, Schug J, Won KJ, Liu C, Naji A, Avrahami D, et al. Single-Cell Transcriptomics of the Human Endocrine Pancreas. *Diabetes.* 2016;65(10):3028-38.

46. Muraro MJ, Dharmadhikari G, Grün D, Groen N, Dielen T, Jansen E, et al. A Single-Cell Transcriptome Atlas of the Human Pancreas. *Cell Syst.* 2016;3(4):385-94.e3.

47. Segerstolpe Å, Palasantza A, Eliasson P, Andersson EM, Andréasson AC, Sun X, et al. Single-Cell Transcriptome Profiling of Human Pancreatic Islets in Health and Type 2 Diabetes. *Cell Metab.* 2016;24(4):593-607.

48. Norris AW, Ode KL, Merjaneh L, Sanda S, Yi Y, Sun X, et al. Survival in a bad neighborhood: pancreatic islets in cystic fibrosis. *J Endocrinol.* 2019;241(1):R35-R50.

49. Hart NJ, Aramandla R, Poffenberger G, Fayolle C, Thames AH, Bautista A, et al. Cystic fibrosis-related diabetes is caused by islet loss and inflammation. *JCI Insight.* 2018;3(8).

50. Sinđić A, Sussman CR, and Romero MF. Primers on molecular pathways: bicarbonate transport by the pancreas. *Pancreatology.* 2010;10(6):660-3.

51. Alka K, and Casey JR. Bicarbonate transport in health and disease. *IUBMB Life.* 2014;66(9):596-615.

52. Park HW, and Lee MG. Transepithelial bicarbonate secretion: lessons from the pancreas. *Cold Spring Harb Perspect Med.* 2012;2(10).

53. Montoro DT, Haber AL, Biton M, Vinarsky V, Lin B, Birket SE, et al. A revised airway epithelial hierarchy includes CFTR-expressing ionocytes. *Nature.* 2018;560(7718):319-24.

54. Plasschaert LW, Žilionis R, Choo-Wing R, Savova V, Knehr J, Roma G, et al. A single-cell atlas of the airway epithelium reveals the CFTR-rich pulmonary ionocyte. *Nature.* 2018;560(7718):377-81.

55. Lieber M, Mazzetta J, Nelson-Rees W, Kaplan M, and Todaro G. Establishment of a continuous tumor-cell line (panc-1) from a human carcinoma of the exocrine pancreas. *Int J Cancer.* 1975;15(5):741-7.

56. Wu Y, Li J, Saleem S, Yee SP, Hardikar AA, and Wang R. c-Kit and stem cell factor regulate PANC-1 cell differentiation into insulin- and glucagon-producing cells. *Lab Invest.* 2010;90(9):1373-84.

57. Gottschalk LB, Vecchio-Pagan B, Sharma N, Han ST, Franca A, Wohler ES, et al. Creation and characterization of an airway epithelial cell line for stable expression of CFTR variants. *J Cyst Fibros.* 2016;15(3):285-94.

58. McIntosh JC, Schoumacher RA, and Tiller RE. Pancreatic adenocarcinoma in a patient with cystic fibrosis. *Am J Med.* 1988;85(4):592.

59. Schoumacher RA, Ram J, Iannuzzi MC, Bradbury NA, Wallace RW, Hon CT, et al. A cystic fibrosis pancreatic adenocarcinoma cell line. *Proc Natl Acad Sci U S A.* 1990;87(10):4012-6.

60. Bockmühl Y, Murgatroyd CA, Kuczynska A, Adcock IM, Almeida OF, and Spengler D. Differential regulation and function of 5'-untranslated GR-exon 1 transcripts. *Mol Endocrinol.* 2011;25(7):1100-10.

61. Babendure JR, Babendure JL, Ding JH, and Tsien RY. Control of mammalian translation by mRNA structure near caps. *RNA.* 2006;12(5):851-61.

62. Bertrand CA, Mitra S, Mishra SK, Wang X, Zhao Y, Pilewski JM, et al. The CFTR trafficking mutation F508del inhibits the constitutive activity of SLC26A9. *Am J Physiol Lung Cell Mol Physiol.* 2017;312(6):L912-L25.

63. Ghazalpour A, Bennett B, Petyuk VA, Orozco L, Hagopian R, Mungrue IN, et al. Comparative analysis of proteome and transcriptome variation in mouse. *PLoS Genet.* 2011;7(6):e1001393.

64. Delaspre F, Beer RL, Rovira M, Huang W, Wang G, Gee S, et al. Centroacinar Cells Are Progenitors That Contribute to Endocrine Pancreas Regeneration. *Diabetes.* 2015;64(10):3499-509.

65. Harris A. The Duct Cell in Cystic Fibrosis. *Annals of the New York Academy of Sciences.* 2006;30(880):17-30.

66. Beer RL, Parsons MJ, and Rovira M. Centroacinar cells: At the center of pancreas regeneration. *Dev Biol.* 2016;413(1):8-15.

67. Ghaye AP, Bergemann D, Tarifeño-Saldivia E, Flasse LC, Von Berg V, Peers B, et al. Progenitor potential of nkx6.1-expressing cells throughout zebrafish life and during beta cell regeneration. *BMC Biol.* 2015;13:70.

68. Boom A, Lybaert P, Pollet JF, Jacobs P, Jijakli H, Golstein PE, et al. Expression and localization of cystic fibrosis transmembrane conductance regulator in the rat endocrine pancreas. *Endocrine.* 2007;32(2):197-205.

69. Huang WQ, Guo JH, Zhang XH, Yu MK, Chung YW, Ruan YC, et al. Glucose-Sensitive CFTR Suppresses Glucagon Secretion by Potentiating KATP Channels in Pancreatic Islet α Cells. *Endocrinology.* 2017;158(10):3188-99.

70. Barry PJ, Banerjee A, Horsley A, and Brennan AL. 182 Impact of ivacaftor on glycaemic health in patients carrying the G551D mutation. *Journal of Cystic Fibrosis.* 2015;14:S104.

71. Kirwan L, Fletcher G, Harrington M, Jeleniewska P, Zhou S, Casserly B, et al. Longitudinal Trends in Real-World Outcomes after Initiation of Ivacaftor. A Cohort Study from the Cystic Fibrosis Registry of Ireland. *Ann Am Thorac Soc.* 2019;16(2):209-16.

72. Hardt PD, Krauss A, Bretz L, Porsch-Ozcürümez M, Schnell-Kretschmer H, Mäser E, et al. Pancreatic exocrine function in patients with type 1 and type 2 diabetes mellitus. *Acta Diabetol.* 2000;37(3):105-10.

73. Nunes AC, Pontes JM, Rosa A, Gomes L, Carvalheiro M, and Freitas D. Screening for pancreatic exocrine insufficiency in patients with diabetes mellitus. *Am J Gastroenterol.* 2003;98(12):2672-5.

74. Raeder H, Johansson S, Holm PI, Haldorsen IS, Mas E, Sbarra V, et al. Mutations in the CEL VNTR cause a syndrome of diabetes and pancreatic exocrine dysfunction. *Nat Genet.* 2006;38(1):54-62.

75. Vesely PW, Staber PB, Hoefler G, and Kenner L. Translational regulation mechanisms of AP-1 proteins. *Mutat Res.* 2009;682(1):7-12.

76. Karin M, Liu Z, and Zandi E. AP-1 function and regulation. *Curr Opin Cell Biol.* 1997;9(2):240-6.

77. Gupta MK, and Vadde R. Identification and characterization of differentially expressed genes in Type 2 Diabetes using in silico approach. *Comput Biol Chem.* 2019;79:24-35.

78. Li J, Li S, Hu Y, Cao G, Wang S, Rai P, et al. The Expression Level of mRNA, Protein, and DNA Methylation Status of. *J Diabetes Res.* 2016;2016:5957404.

79. Huda N, Hosen MI, Yasmin T, Sarkar PK, Hasan AKMM, and Nabi AHMN. Genetic variation of the transcription factor GATA3, not STAT4, is associated with the risk of type 2 diabetes in the Bangladeshi population. *PLoS One.* 2018;13(7):e0198507.

80. Gao N, Le Lay J, Qin W, Doliba N, Schug J, Fox AJ, et al. Foxa1 and Foxa2 maintain the metabolic and secretory features of the mature beta-cell. *Mol Endocrinol.* 2010;24(8):1594-604.

81. Vatamaniuk MZ, Gupta RK, Lantz KA, Doliba NM, Matschinsky FM, and Kaestner KH. Foxa1-deficient mice exhibit impaired insulin secretion due to uncoupled oxidative phosphorylation. *Diabetes.* 2006;55(10):2730-6.

82. Manolio TA, Collins FS, Cox NJ, Goldstein DB, Hindorff LA, Hunter DJ, et al. Finding the missing heritability of complex diseases. *Nature.* 2009;461(7265):747-53.

83. Sondo E, Caci E, and Galietta LJ. The TMEM16A chloride channel as an alternative therapeutic target in cystic fibrosis. *Int J Biochem Cell Biol.* 2014;52:73-6.

84. Muraglia KA, Chorghade RS, Kim BR, Tang XX, Shah VS, Grillo AS, et al. Small-molecule ion channels increase host defences in cystic fibrosis airway epithelia. *Nature.* 2019;567(7748):405-8.

85. Balázs A, and Mall MA. Role of the SLC26A9 Chloride Channel as Disease Modifier and Potential Therapeutic Target in Cystic Fibrosis. *Front Pharmacol.* 2018;9:1112.

86. Mall MA, and Galietta LJ. Targeting ion channels in cystic fibrosis. *J Cyst Fibros.* 2015;14(5):561-70.

87. Vecchio-Pagán B, Blackman SM, Lee M, Atalar M, Pellicore MJ, Pace RG, et al. Deep resequencing of *CFTR* in 762 F508del homozygotes reveals clusters of non-coding variants associated with cystic fibrosis disease traits. *Hum Genome Var.* 2016;3:16038.

88. Purcell S, Neale B, Todd-Brown K, Thomas L, Ferreira MA, Bender D, et al. PLINK: a tool set for whole-genome association and population-based linkage analyses. *Am J Hum Genet.* 2007;81(3):559-75.

89. Pruim RJ, Welch RP, Sanna S, Teslovich TM, Chines PS, Gliedt TP, et al. LocusZoom: regional visualization of genome-wide association scan results. *Bioinformatics.* 2010;26(18):2336-7.

90. Lee S, Wu MC, and Lin X. Optimal tests for rare variant effects in sequencing association studies. *Biostatistics.* 2012;13(4):762-75.

91. Langmead B, and Salzberg SL. Fast gapped-read alignment with Bowtie 2. *Nat Methods.* 2012;9(4):357-9.

92. Trapnell C, Pachter L, and Salzberg SL. TopHat: discovering splice junctions with RNA-Seq. *Bioinformatics.* 2009;25(9):1105-11.

93. Trapnell C, Hendrickson DG, Sauvageau M, Goff L, Rinn JL, and Pachter L. Differential analysis of gene regulation at transcript resolution with RNA-seq. *Nat Biotechnol.* 2013;31(1):46-53.

94. Behre G, Smith LT, and Tenen DG. Use of a promoterless Renilla luciferase vector as an internal control plasmid for transient co-transfection assays of Ras-mediated transcription activation. *Biotechniques.* 1999;26(1):24-6, 8.

95. Sherf B, Navarro S, Hannah R, and Wood K. Dual-Luciferase Reporter Assay: An Advanced Co-Reporter Technology Integrating Firefly and Renilla Luciferase Assays. 1996;57:2–8.

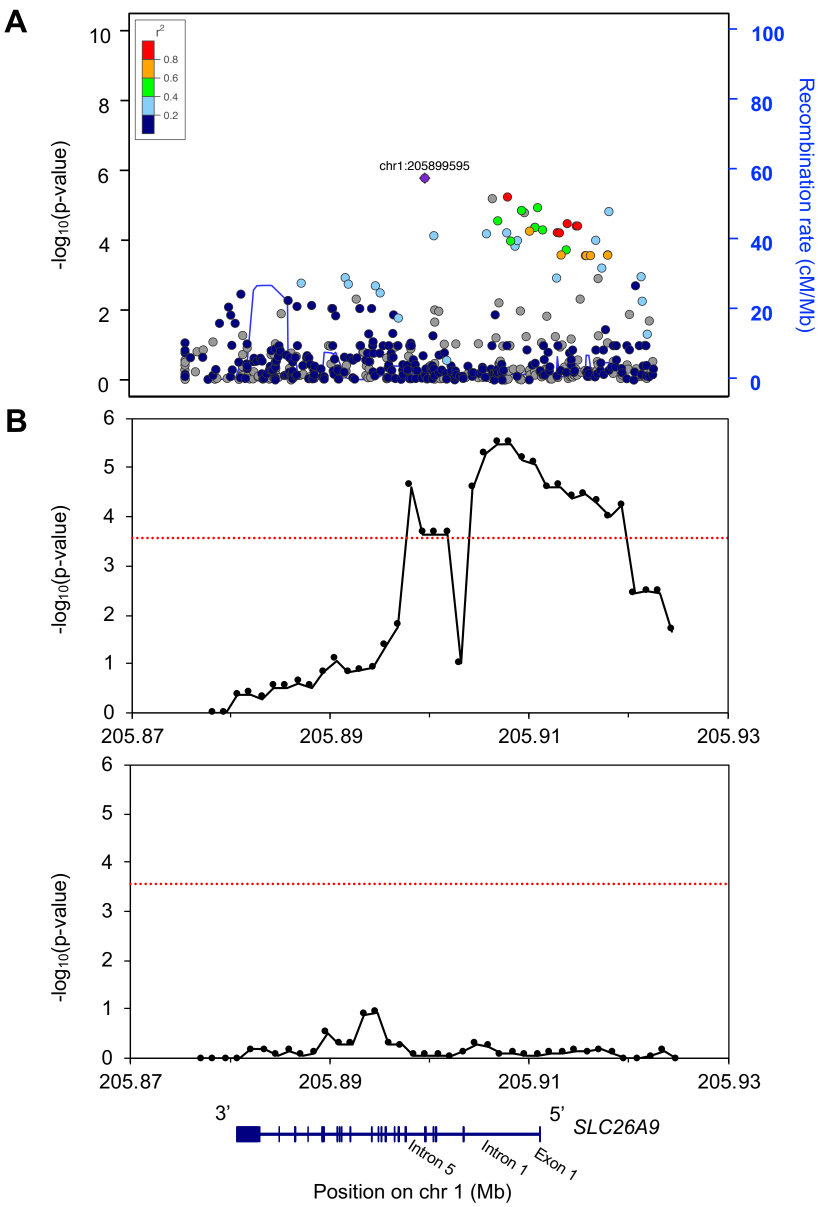

Figure 1. Association of *SLC26A9* variants with age-at-onset of CFRD in 762 p.Phe508del (F508del) homozygous individuals. Variants within a 47.7 kb region encompassing *SLC26A9* (shown to scale at bottom) were tested. (**A**) Manhattan plot for association with CFRD (points, left y-axis) and recombination ratio plotted by genomic location (blue line, right y-axis). (**B**) SKAT-O test for association of sets of common (top) and rare (bottom) variants with CFRD. All variants within each 5 kb window, moved across the entire region in increments of 1,250 bp, were tested for a combined association with CFRD via SKAT-O test. The *x*-axis denotes position on chromosome 1 (hg19), *y*-axis is −log10 of the regional *p*-value. Association values were plotted at the center of each 5 kb window. Common and rare variants were assigned based on a MAF cut-off of 1%. Red line indicates significance threshold Bonferroni corrected for the number of sliding windows (p=0.01/36=2.7E-4). No other RefSeq genes are present in this region other than *SLC26A9*.

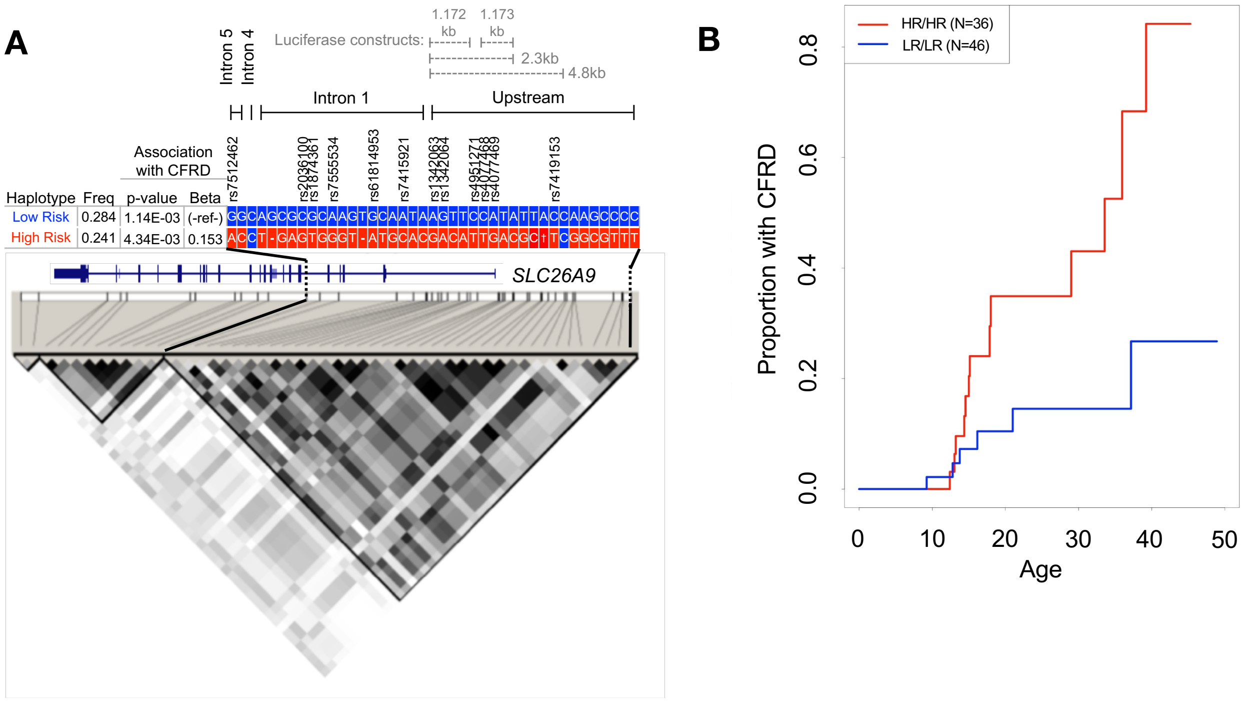

Figure 2. Two common haplotypes that associate with age-at-onset of CFRD. (**A**) **Top:** *SLC26A9* variant haplotypes with MAF>15% and MHF>20%. Location of variants relative to *SLC26A9* and the luciferase constructs are shown above haplotypes (Note: *SLC26A9* is on (-) DNA strand, not drawn to scale). † indicates TGGGGCCTCGGGTATCTCA. Haplotype frequencies, p-values and beta values are shown to the left of the respective haplotype. rsIDs are shown for the CFRD-associated variants (8). Variants highlighted in blue indicate alleles composing the most common ancestral haplotype. Variants highlighted in red indicate alleles that differ from those in the common haplotype. **Bottom:** LD plot of variants with MAF>15% created with Haploview. Black boxes indicate an r^2 value of 1 or complete LD, while white boxes indicate an r^2 of 0 or linkage equilibrium. Proposed LD blocks are outlined (triangles), defined by a recombination event between intron 5 and 8. (**B**) Cumulative Incidence plot of proportion with CFRD relative to age among individuals with low risk (LR) or high risk (HR) haplotypes. LR/LR homozygotes (n=46) versus HR/HR homozygotes (n=36) are plotted (log-rank p-value: 6.5E-3).

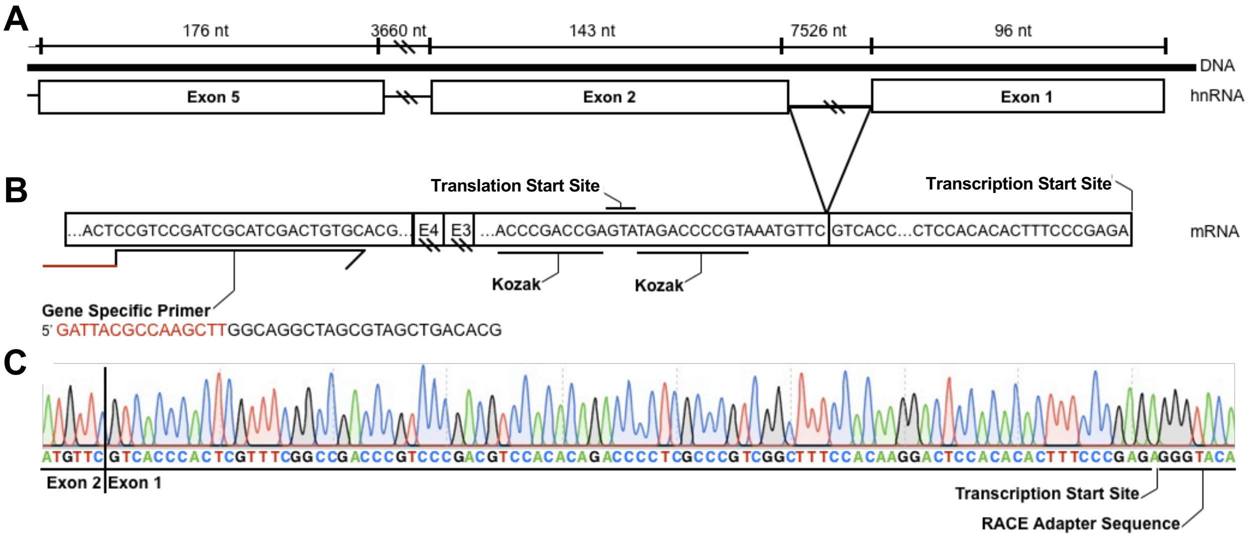
A
176 nt
3660 nt
143 nt
7526 nt
96 nt
DNA
Exon 5
Exon 2
Exon 1
hnRNA
B
Translation Start Site
Transcription Start Site
...ACTCCGTCCGATCGCATCGACTGTGCACG...
E4
E3
...ACCCGACCGAGTATAGACCCCGTAAATGTTC
GTCACC...CTCCACACACTTTCCCGAGA
mRNA
Kozak
Kozak
Gene Specific Primer
5' GATTACGCCAAGCTTGGCAGGCTAGCGTAGCTGACACG
C
ATGTTCGTCACCCACTCGTTTCGGCCGACCCGTCCCGACGTCCACACAGACCCCTCGCCCGTCGGCTTTCCACAAGGACTCCACACACTTTCCCGAGAGGGTACA
Exon 2
Exon 1
Transcription Start Site
RACE Adapter Sequence

Figure 3. Transcription Start Site of *SLC26A9* in pancreas. (**A**) Schematic in native orientation showing the first five exons of the *SLC26A9* gene. Note: *SLC26A9* is transcribed from the minus strand. The size of exon and intron regions are labeled (nt). The hash marks denote where the figure is not drawn to scale. (**B**) Summary of sequence of 5' RACE obtained from one primary human pancreas RNA. 5' RACE was performed using a gene specific primer (GSP) in exon 5 of *SLC26A9*. The portion of the GSP in red is the overhang necessary for Infusion PCR. Transcription start site (TSS) marks the beginning of exon 1. The translational start site with the Kozak consensus sequence occurs in exon 2. (**C**) Sanger sequencing trace of the 5' RACE product from the *SLC26A9* mRNA transcripts in human pancreas. Upstream of the TSS is the RACE adapter sequence confirming the 5' most extent of the RACE product. The sequencing trace crosses exon-exon junctions (shown here between exon 1 and 2 by the vertical black line) confirming that RACE used mRNA as the template. Sanger sequencing of 5' RACE products obtained from primary human lung (N=3) and stomach (N=1) samples identified the same TSS (not shown).

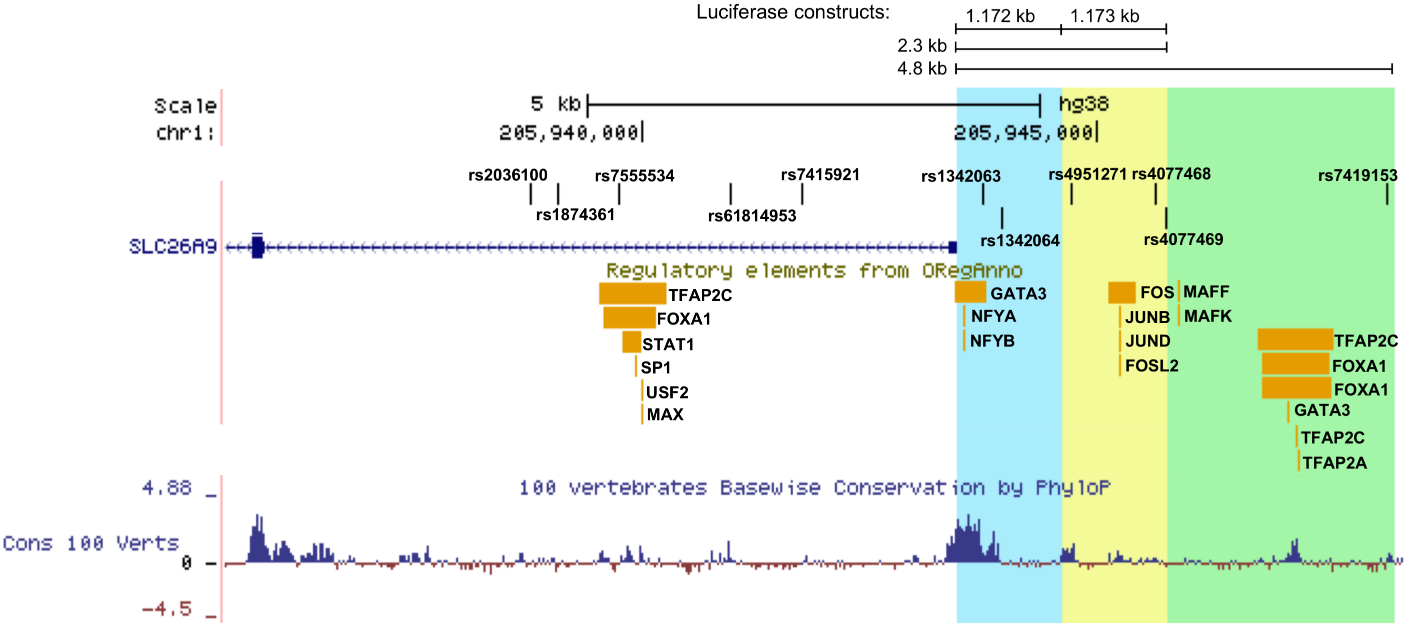

Figure 4. Regulatory annotations 5' and within *SLC26A9* from the UCSC Genome Browser. The key CFRD-risk variants (8) 5' and within *SLC26A9* are annotated at the top. The blue region highlights the 1.172 kb region 5' of *SLC26A9.* The yellow region highlights the 1.173 kb region that together with the blue region denotes the 2.3 kb region 5' of *SLC26A9.* The green highlight denotes the 2.5 kb region, which encompasses the rest of the 5' 4.8 kb region upstream of *SLC26A9.* The ORegAnno track displays transcription factor binding sites. The bottom track displays the Vertebrate Multiz Alignment & Conservation.

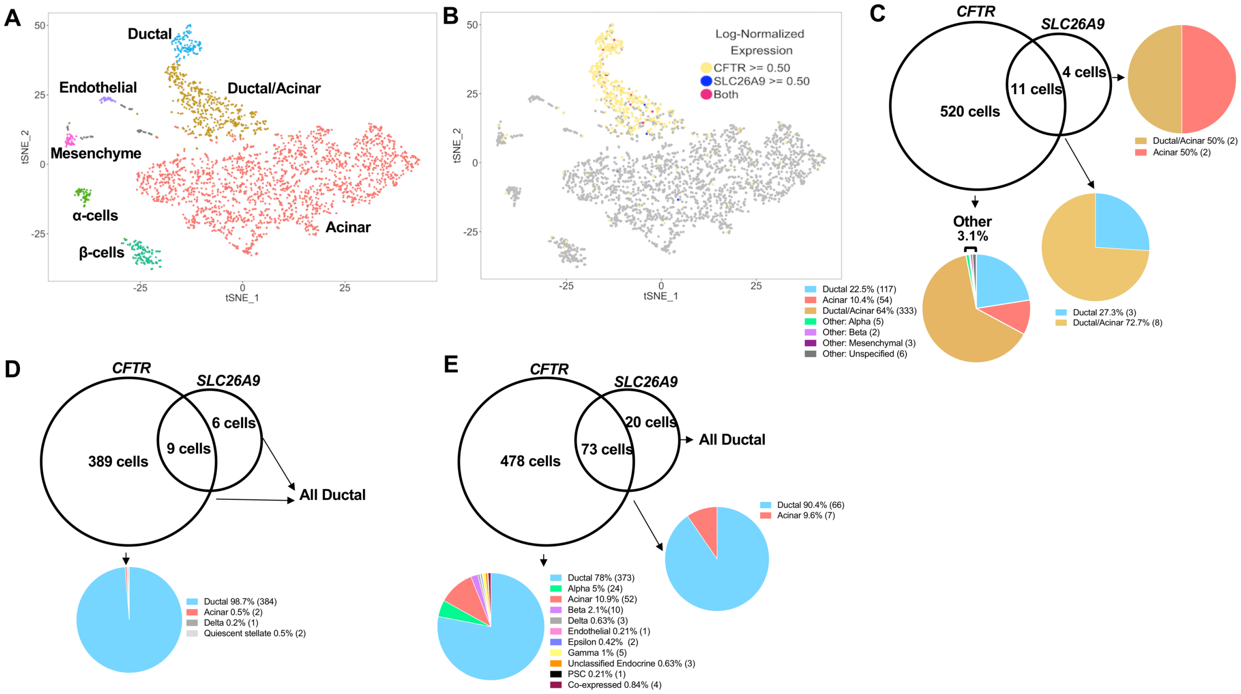

Figure 5 Co-expression of *SLC26A9* and *CFTR* in pancreatic cells. Results were obtained from scRNA-seq. (**A**) t-SNE plot of scRNA-seq data. Each data point represents a cell, colored by its cell type. (**B**) t-SNE plot of scRNA-seq of the pancreas, with cells expressing *CFTR* and/or *SLC26A9* with a log-normalized expression ≥0.50 are colored (**C**) Venn diagram representing the number of cells that express *CFTR*, *SLC26A9*, or both, and the percentage of cell types in which these genes are expressed. The number of cells per compartment are shown in parentheses. (**D**) and (**E**) Venn diagrams showing the number of cells expressing *CFTR*, *SLC26A9* or both and the percentage of cell types in which these genes are expressed based upon a reanalysis of two publicly available scRNA-seq datasets (44, 47).

scRNA-seq (n=2,999)				PANC-1 RNA-seq (n=5)	CFPAC-1 RNA-seq (n=1)
Gene B	Cells expressing Gene B (Ductal/Ductal Acinar)	Proportion of SLC26A9-expressing cells that express Gene B (Ductal/Ductal Acinar)	Significance of co-expression (p-value)	Gene expression (FPKM)	
CFTR	531 (461)	11(11) / 15(13) [73.4%]	2.31E-07	0.02	0.04
FOS	2633 (599)	15(13) / 15(13) [100%]	<2.2e-16	54.94	325.72
JUND	2251 (568)	14(12) / 15(13) [93.4%]	1.34E-02	56.17	123.31
JUNB	935 (340)	11(10) / 15(13) [73.4%]	1.34E-04	64.71	218.20
FOSL2	284 (91)	4(4) / 15(13) [26.7%]	9.95E-03	12.95	9.26
SP1	101 (51)	3(3) / 15(13) [20%]	1.24E-03	24.48	29.12
MAFK	275 (144)	(3) / 15(13) [20%]	4.20E-02	50.66	17.88
STAT1	181 (96)	2(2) / 15(13) [13.4%]	5.75E-02	44.41	66.18
NFYA	32 (22)	1(1) / 15(13) [6.7%]	1.06E-02	14.2	10.11
NFYB	139 (63)	1(1) / 15(13) [6.7%]	1.51E-01	14.25	5.02
MAX	156 (59)	1(1) / 15(13) [6.7%]	1.82E-01	23.3	42.68
USF2	265 (84)	1(1) / 15(13) [6.7%]	3.88E-01	72.65	40.46
MAFF	296 (202)	1(1) / 15(13) [6.7%]	4.44E-01	5.52	46.05
GATA3	0 (0)	0(0) / 15(13) [0%]	NA	3.57	17.50
TFAP2A	0 (0)	0(0) / 15(13) [0%]	NA	34.61	55.62
FOXA1	3 (2)	0(0) / 15(13) [0%]	NA	1.55	10.58
TFAP2C	7 (2)	0(0) / 15(13) [0%]	NA	3.15	1.82

Table 1. Expression of transcription factors and CFTR in the pancreas, PANC-1 and CFPAC-1 cells. Number of cells co-expressing *SLC26A9* and other genes in the pancreas was quantified using scRNA-seq. Cells were determined to express the respective gene for normalized log-transformed gene expression > 0.5. Number of ductal and ductal/acinar cells expressing respective gene are shown in parenthesis. Fraction of cells co-expressing *SLC26A9* and respective gene are shown in brackets. Significance of the co-expression of two genes were determined with a hypergeometric test. NA indicates that a significance test was not applicable. Rightmost column indicates average gene expression in PANC-1 and CFPAC-1 cells determined by publicly available RNA-sequencing data. *SLC26A9* is expressed in PANC-1 and CFPAC-1 cells with 0.01 and 3.0003 FPKM, respectively.

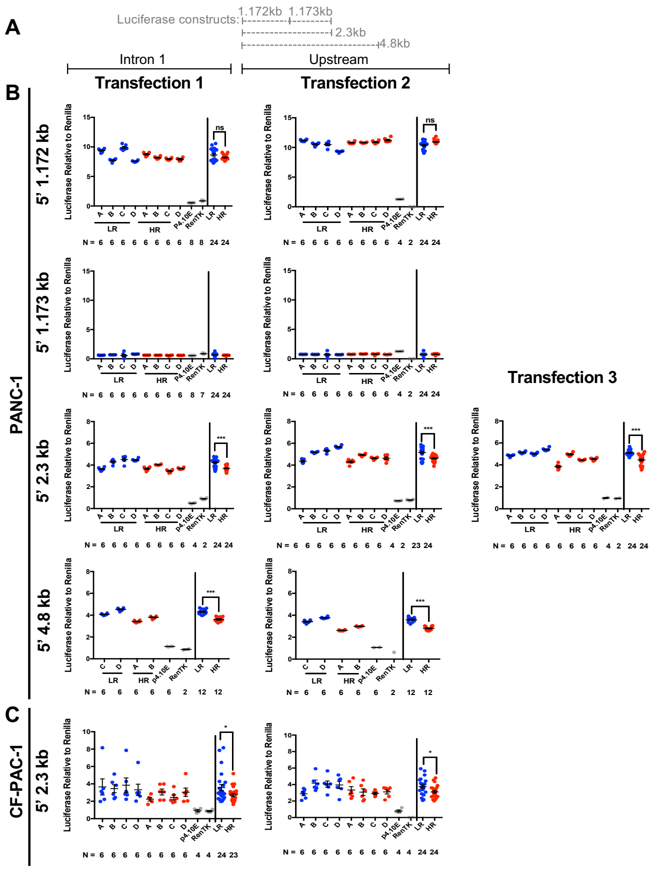

Figure 6. Reporter gene expression driven by DNA fragments derived from the 5' region of *SLC26A9.* (**A**) Diagram depicting the location and length of the regions studied relative to *SLC26A9*. (**B**) Luciferase expression levels obtained from PANC-1 cells transfected with various *SLC26A9* DNA fragments bearing either LR or HR risk variants for CFRD. The 1.172 kb region generated robust expression of luciferase consistent with a promoter. Levels do not differ between the LR and HR bearing fragments. The 1.173 kb region generated little to no activity, similar to negative controls. The 2.3 kb region composed of the 1.172 kb and 1.173 kb region generated a combined expression of luciferase that was 12% higher for LR compared to HR haplotype (p-value: 5.15E-09)**.** The 4.8kb region generated a combined 19% higher expression level compared to HR (p-value: 6.28E-07)**.** (**C**) Transfections in CFPAC-1 cells resulted in same trend being observed. The 2.3 kb region drove a combined expression of luciferase that was 20% higher for LR compared to HR haplotype (p-value 2.00E-03). **For plots in (B) and (C):** Results are shown for 2-3 separate transfections of PANC-1 and CFPAC-1 cells with 2-4 independent plasmid constructs (A-D); each containing alleles corresponding to the LR (blue) or HR (red) haplotypes in their native orientation. For each transfection, the data points to the left of the vertical line are results from each independent clone. On the right, data points from all clones are combined and asterisks indicate significance (* = p-value ≤0.05; *** = p-value ≤0.001). Negative controls (pGL4.10 empty vector and renilla) are shown in gray. Total data points (N) are listed below each construct. Significance was assessed using Student's t-test. Error bars with SEM.

	Baron(n=8,569)			Wang(n=635)			Muraro(n=3,072)			Segerstolpe(n=2,209)		
Gene B	**Cells expressing Gene B (Ductal)**	**Proportion of *SLC26A9*-expressing cells that express Gene B (Ductal) [%]**	**Significance of co-expression (p-value)**	**Cells expressing Gene B**	**Proportion of *SLC26A9*-expressing cells that express Gene B [%]**	**Significance of co-expression (p-value)**	**Cells expressing Gene B**	**Proportion of *SLC26A9*-expressing cells that express Gene B [%]**	**Significance of co-expression (p-value)**	**Cells expressing Gene B (Ductal)**	**Proportion of *SLC26A9*-expressing cells that express Gene B (Ductal) [%]**	**Significance of co-expression (p-value)**
CFTR	389 (384)	9 (9) / 15 (15) [60%]	1.02E-23	348	16/19 [84.3%]	1.27E-03	604	28/34 [82.4%]	1.92E-16	478 (373)	73 (66) / 93 (66) [78.5%]	3.16E-34
FOS	3855 (591)	13 (13) / 15 (15) [86.7%]	2.53E-03	613	19/19 [100%]	<2.2e-16	1848	24/34 [70.6%]	7.46E-02	1215 (244)	61 (37) / 93 (66) [65.6%]	1.31E-02
JUND	5354 (768)	11 (11) / 15 (15) [73.3%]	2.26E-02	618	19/19 [100%]	<2.2e-16	1851	27/34 [79.5%]	4.97E-03	1752 (327)	86 (60) / 93 (66) [92.5%]	1.08E-04
JUNB	5300 (844)	11 (11) / 15 (15) [73.3%]	4.97E-01	465	10/19 [52.7%]	9.59E-01	1848	25/34 [73.6%]	3.47E-02	1660 (330)	78 (56) / 93 (66) [83.9%]	1.41E-02
FOSL2	954 (278)	5 (5) / 15 (15) [33.3%]	2.33E-04	103	5/19 [26.4%]	7.09E-02	514	19/34 [55.9%]	2.90E-08	372 (206)	57 (42) / 93 (66) [61.3%]	5.29E-24
SP1	168 (53)	0 (0) / 15 (15) [0%]	NA	390	16/19 [84.3%]	6.96E-03	1381	30/34 [88.3%]	1.58E-08	823 (213)	61 (45) / 93 (66) [65.6%]	4.07E-09
MAFK	257 (102)	2 (2) / 15 (15) [13.3%]	2.25E-02	133	6/19 [31.6%]	8.02E-02	28	0/34 [0%]	NA	123 (41)	11 (9) / 93 (66) [11.8%]	4.53E-03
STAT1	624 (101)	2 (2) / 15 (15) [13.3%]	1.40E-02	457	15/19 (78.9%)	1.73E-01	1873	32/34 [94.1%]	1.02E-06	1511 (326)	77 (58) / 93 (66) [82.8%]	4.36E-04
NFYA	51 (16)	0 (0) / 15 (15) [0%]	NA	285	8/19 [42.2%]	5.02E-01	770	22/34 [64.8%]	1.78E-07	704 (200)	56 (43) / 93 (66) [60.2%]	2.35E-09
NFYB	165 (17)	0 (0) / 15 (15) [0%]	NA	261	5/19 [26.4%]	8.64E-01	923	20/34 [58.9%]	1.17E-04	863 (196)	58 (44) / 93 (66) [62.4%]	1.05E-06
MAX	555 (70)	1 (1) / 15 (15) [6.7%]	9.82E-01	243	6/19 [31.6%]	6.38E-01	1516	23/34 [67.7%]	9.63E-03	1314 (294)	77 (56) / 93 (66) [82.8%]	2.14E-07
USF2	1339 (132)	2 (2) / 15 (15) [13.3%]	5.42E-01	226	7/19 [36.9%]	3.53E-01	718	9/34 [26.5%]	2.57E-01	1302 (196)	45 (27) / 93 (66) [48.4%]	9.77E-01
MAFF	595 (264)	3 (3) / 15 (15) [20%]	9.77E-06	147	9/19 [47.4%]	4.37E-03	602	16/34 [47.1%]	6.14E-05	471 (174)	33 (30) / 93 (66) [35.5%]	4.14E-04
GATA3	1 (0)	0 (0) / 15 (15) [0%]	NA	2	0/19 [0%]	NA	8	1/34 [3%]	3.19E-03	8 (3)	1 (1) / 93 (66) [1.1%]	4.16E-02
TFAP2A	11 (10)	0 (0) / 15 (15) [0%]	NA	9	2/19 [10.6%]	1.71E-03	41	5/34 [14.8%]	3.95E-06	67 (46)	9 (7) / 93 (66) [9.7%]	3.65E-04
FOXA1	10 (5)	0 (0) / 15 (15) [0%]	NA	21	0/19 [0%]	NA	94	4/34 [11.8%]	3.32E-03	37 (10)	4 (3) / 93 (66) [4.3%]	1.78E-02
TFAP2C	4 (1)	0 (0) / 15 (15) [0%]	NA	10	1/19 [5.3%]	3.31E-02	56	4/34 [11.8%]	3.12E-04	31 (15)	9 (7) / 93 (66) [9.7%]	2.30E-07

Table 2. *SLC26A9* and relevant gene expression in pancreatic cells. Results were derived from 4 scRNA-seq datasets involving 31 subjects downloaded from the gene expression omnibus repository (accession numbers GSE84133, GSE83139, GSE85241) and the ArrayExpress (EBI) (E-MTAB-5061). Number of cells expressing respective genes are listed, with the number of ductal cells expressing that gene listed in parentheses. Fraction of cells co-expressing *SLC26A9* and respective gene are shown in brackets. Cells were determined to express respective gene for gene count >1. Significance of the co-occurrence of two genes were determined with a hypergeometric test. NA indicates that a significance test was not applicable.